



1 Greenhouse gas fluxes in mangrove forest soil in the Amazon estuary

2 Saúl Edgardo Martínez Castellón¹, José Henrique Cattanio^{1*}, José Francisco Berrêdo^{1,3},
3 Marcelo Rollnic², Maria de Lourdes Ruivo^{1,3}, Carlos Noriega².

4 ¹ Graduate Program in Environmental Sciences. Federal University of Pará, Belém,
5 Brazil

6 ² Marine Environmental Monitoring Research Laboratory. Federal University of Pará,
7 Belém, Brazil.

8 ³ Department of Earth Sciences and Ecology. Paraense Emílio Goeldi Museum, Belém,
9 Brazil

10 * Corresponding author: cattanio@ufpa.br (J.H. Cattanio)

11 Abstract: Tropical mangrove forests are important carbon sinks, the soil being the main
12 reservoir of this chemical element. Understanding the variability and the key factors that
13 control fluxes is critical to account for greenhouse gas (GHG) emissions, especially in a
14 scenario of global climate change. The current study is the first to quantify methane
15 (CH₄) and carbon dioxide (CO₂) emissions using a dynamic chamber in Amazon natural
16 mangrove soils. Sampling points were selected in a contrasting topographic gradient,
17 the highest point being where flooding occurs only at high tides during the solstice and
18 on the high tides of the rainy season of the new and full moons. The results showed that
19 mangrove soils are sources of greenhouse gases, and CO₂ fluxes were not different
20 between seasons, and only in the dry period were they greater in the high topography.
21 Only in the low topography, the CH₄ fluxes were higher in the rainy season. However,
22 in the dry period, the low topography soil produced more CH₄. Soil organic matter,
23 carbon and nitrogen ratio (C/N), and redox potential influenced the annual and seasonal
24 variation of CO₂ emissions; however, they did not influence CH₄ flux. To account for
25 global GHG emissions, in the Amazonian estuary mangrove soil produced 35.4 Mg
26 CO_{2-eq} ha⁻¹ yr⁻¹.

27 1 Introduction

28 The Amazon coastal areas in the State of Pará (Brazil) cover 2,176.8 km² where
29 mangroves develop under the macro-tide regime in the (Souza Filho, 2005),
30 representing approximately 85% of the entire area of Brazilian mangroves (Herz, 1991).
31 These mangrove areas are estimated to be the main contributors to greenhouse gas
32 emissions in marine ecosystems (Allen et al., 2011; Chen et al., 2012). However,
33 mangrove forests are highly productive due to a high nutrient turnover rate (Robertson
34 et al., 1992) and have mechanisms that maximize carbon gain and minimize water loss
35 through plant transpiration (Alongi and Mukhopadhyay, 2015). A study conducted in 25



36 mangrove forests (between 30° latitude and 73° longitude) revealed that these forests
37 are the richest in carbon storage in the tropics, containing on average 1023 Mg C ha⁻¹ of
38 which 49 to 98% is present in the soil (Donato et al., 2011). In addition, phenolic
39 compounds inhibit microbial activity and help keep organic carbon intact, thus
40 accumulating organic matter in mangrove forest soils (Friesen et al., 2018).

41 The production of greenhouse gases from soils is mainly attributable to biogeochemical
42 processes. Microbial activities and gas production are related to soil properties,
43 including total carbon and total nitrogen concentrations, moisture, porosity, salinity, and
44 redox potential (Bouillon et al., 2008; Chen et al., 2012). Due to the dynamics of tidal
45 movements, mangrove soils may become saturated and present a reduced oxygen
46 availability or total aeration caused by the ebb tide. Studies attribute soil carbon flux
47 responses to moisture perturbations because of seasonality and flooding events
48 (Banerjee et al., 2016), with fluxes being dependent on tidal extremes (high tide and low
49 tide), and flood duration (Chowdhury et al., 2018).

50 The estimated CO₂ production to the atmosphere, in tropical estuarine areas, is 16.2
51 TgCy⁻¹ (Alongi, 2009). However, the most recent estimate between latitude 0° to 23.5°
52 S reveals an emission of 2.3 g CO₂ m⁻² d⁻¹ (Rosentreter et al., 2018a). In situ CO₂
53 production is related to the water input of terrestrial, riparian, and groundwater brought
54 by rainfall (Rosentreter et al., 2018c).

55 Due to this periodic tidal influence, the mangrove ecosystem is regularly flooded,
56 leaving the soil anoxic and reduced, favoring methanogenesis (Dutta et al., 2013). Thus,
57 estuaries are considered hot spots for CH₄ production and emission (Bastviken et al.,
58 2011; Borges et al., 2015). The organic material decomposition by methanogenic
59 bacteria in anoxic environments, such as sediments, inner suspended particles,
60 zooplankton gut (Reeburgh, 2007; Valentine, 2011), and the reduction of sulfate in
61 anoxic marine sediments (Purvaja et al., 2004), also results in CH₄ formation. On the
62 other hand, an ecosystem with salinity levels greater than 18 ppt may show an absence
63 of CH₄ emissions (Poffenbarger et al., 2011). Currently the uncertainties in emitted CH₄
64 values in vegetated coastal wetlands are approximately 30% (EPA, 2017). The total
65 emission of 0.010 Tg CH₄ y⁻¹ or 0.64 g CH₄ m⁻² d⁻¹ was estimated between 0 and 5°
66 latitude (Rosentreter et al., 2018a).

67 The objective of this study is to investigate the spatial and seasonal variation in the
68 monthly fluxes of CO₂ and CH₄ from the soil in a non-anthropized mangrove area in the

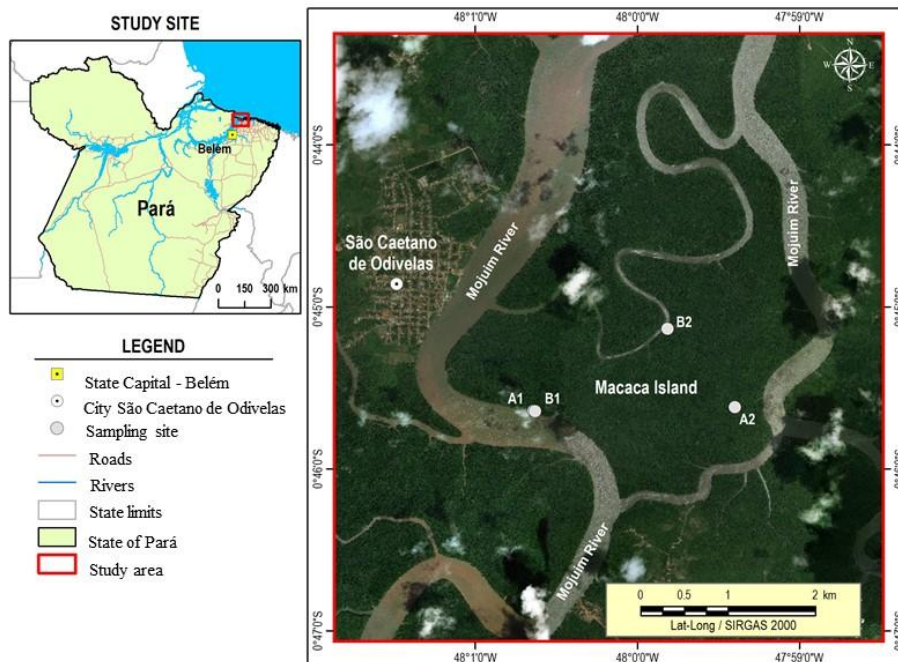


69 Mojuim River Estuary, belonging to the Amazon biome. The environmental factors and
70 physicochemical analysis of the soil were investigated from 2017 to 2018 to understand
71 the gas fluxes.

72 **2 Material and Methods**

73 2.1 Study site

74 This study was conducted in the Amazonian coastal zone, Macaca Island, located in the
75 Mojuim River estuary, at the Mocapajuba Marine Extractive Reserve, municipality of
76 São Caetano de Odivelas (Figure 1), state of Pará (Brazil). Macaca island has an area of
77 1,322 ha with exclusively untouched mangrove forests, which belongs to a coastal strip
78 of 2177 km² in the state of Pará (Souza Filho, 2005). The climate is Am type according
79 to the Köppen classification (Peel et al., 2007). The climatological data were obtained
80 from the Meteorological Database for Teaching and Research of the National Institute
81 of Meteorology (INMET). The area has a rainy season from January to June (2,296 mm
82 of precipitation) and a dry season from July to December (687 mm). March and April
83 are the rainiest months with 505 and 453 mm of precipitation, while October and
84 November are the driest (53 and 61 mm, respectively). The minimum temperatures
85 occur in the rainy period (26 °C) and the maximum in the dry period (29 °C). The
86 Mojuim estuary has a macrotidal regime, with an average height of 4.9 m during spring
87 tide and 3.2 m during low tide (Rollnic et al., 2018). During the wet season the Mojuim
88 River has a flow velocity of 1.8 m s⁻¹ at the ebb tide and 1.3 m s⁻¹ at the flood tide.
89 During the dry season, the maximum currents are 1.9 m s⁻¹ at the flood and 1.67 m s⁻¹ at
90 the ebb tide (Rocha, 2015) The annual mean salinity is 26.95 ± 0.98 PSU (Valentim et
91 al., 2018).



92

93 Figure 1. Macaca Island located in the mangrove coast of Northern Brazil, Municipality
94 of São Caetano de Odivelas (state of Pará), with the sampling points at low (B1 and B2)
95 and high topographies (A1 and A2). Image Source: © Google Earth

96 The Mojuim River region is geomorphologically formed by partially submerged river
97 basins consequent of an increase in the relative sea level during the Holocene (Prost et
98 al., 2001) associated with the formation of mangroves, dunes, and beaches (El-Robrini
99 et al., 2006). This river forms the entire watershed of the municipality of São Caetano
100 de Odivelas and borders the municipality of São João da Ponta (Figure 1). Before
101 reaching the estuary, the Mojuim River crosses an area of a dryland forest highly
102 fragmented by family farming, forming remnants of secondary forest (< 5.0 ha) with
103 various ages (Fernandes and Pimentel, 2019). The population economically exploited
104 the estuary, primarily by artisanal fishing, crab (*Ucides cordatus* L.) extraction, and
105 oyster farms.

106 Four sampling sites were selected in the Macaca Island: two where flooding occurs
107 every day (B1 and B2; Figure 1), called low topography, and two where flooding occurs
108 only at high tides during the solstice and on the high tides of the rainy season of the new
109 and full moons (A1 and A2; Figure 1), called high topography. Once a month, the gas



110 flux for each chamber was measured during periods of waning or crescent moon, as
111 these are the times when the soil in the low topography is more exposed. The flora of
112 the mangrove area on the Macaca Island is little anthropized and comprises the genera
113 *Rhizophora*, *Avicenia*, *Laguncularia*, and *Acrostichum* (Ferreira, 2017; França et al.,
114 2016). The estuarine plains are influenced by a macro tide dynamics and can be
115 physiographically divided into four sectors (França et al., 2016). The Macaca Island is
116 classified as being from the fourth sector, which consists of woods of adult trees of the
117 genus *Rhizophora* with an average height of 10 to 25 m, located at an elevation of 0 to 5
118 m, with silt-clay soil (França et al., 2016).

119 2.2 Vegetation structure and biomass

120 The floristic survey was conducted at the same sites as the gas flow study, using circular
121 plots of 1,256.6 m² (Kauffman et al., 2013), divided into four subplots of 314.15 m²,
122 which is the equivalent to 0.38 ha (Figure 1). All trees with DBH (diameter at breast
123 height) greater than 0.05m had their diameter above the aerial roots, the diameter of the
124 stem, and total height recorded. The allometric equation to calculate tree biomass
125 (AGB) was: $AGB = 0.168 \times \rho \times (DBH) \times 2.471$, where ρ represents wood density,
126 using 0.87 g cm⁻³ for *R. mangle* and 0.72 g cm⁻³ for *A. germinans* (Howard et al.,
127 2014b).

128 2.3 Soil sampling and environmental characterization

129 In July 2017 and January 2018, four soil samples were collected with an auger at a
130 depth of 0.10 m in all the studied sites (Figure 1). Before the soil samples were
131 removed, pH and redox potential (Eh; mV) were measured with a Metrohm 744
132 equipment by inserting the platinum probe directly into the soil at a depth of 0.10 m
133 (Bauza et al., 2002). The soil samples were properly stored and taken to the Chemical
134 Analysis Laboratory of the *Museu Paraense Emílio Goeldi*. Salinity (Sal; ppt) was
135 measured with PCE-0100, and soil moisture (Sm; %) by the residual gravimetric
136 method (EMBRAPA, 1997).

137 Organic Matter (OM; g kg⁻¹), Total Carbon (TC; g kg⁻¹) and Total Nitrogen (TN; g kg⁻¹)
138 were calculated by volumetry (oxidoreduction) using the Walkley-Black method
139 (Kalembasa and Jenkinson, 1973). Microbial carbon (Cmic; mg kg⁻¹) and microbial
140 nitrogen (Nmic; mg kg⁻¹) were determined through the 2,0 min of Irradiation-extraction
141 method of soil by microwave technique (Islam and Weil, 1998). Microwave heated soil



142 extraction proved to be a simple, fast, accurate, reliable and safe method to measure soil
143 microbial biomass (Araujo, 2010; Ferreira et al., 1999; Monz et al., 1991). The Cmic
144 was determined by dichromate oxidation (Kalembasa and Jenkinson, 1973; Vance et al.,
145 1987). The Nmic was analyzed following the method described by Brookes et al.
146 (1985), changing fumigation to irradiation, which uses the difference between the
147 amount of TN in irradiated and non-irradiated soil. We used the flux conversion factor
148 of 0.33 (Sparling and West, 1988) and 0.54 (Almeida et al., 2019; Brookes et al., 1985),
149 for carbon and nitrogen, respectively. Particle size analysis was performed separately on
150 four soil samples collected at each flux site, in the two seasons, according to
151 EMBRAPA (1997). .

152 At each flow measurement, environmental variables such as air temperature (T_{air} , °C),
153 relative humidity (RH, %), wind speed (W_s , $m\ s^{-1}$) were quantified with a portable
154 thermo-hygrometer (model AK821) at the height of 2.0 m above the soil surface. Soil
155 temperature (T_s , °C) was measured with a portable digital thermometer (model TP101)
156 sequentially after each flow measurement. Daily precipitation was obtained from an
157 automatic precipitation station installed at a pier on the banks of the Mojuim River in
158 São Caetano das Odivelas (coordinates: 0°44'18.48 "S; 48°00'47.94 "W).

159 2.4 Fluxes Measurements

160 In each plot, eight Polyvinyl Chloride rings with 0.20 m diameter and 0.12 m height
161 were randomly installed within a circumference with a diameter of 20 m. The rings had
162 an area of 0.028 m^2 (volume of 3.47 L) and were fixed 0.05 m into the ground. The
163 height of the ring above ground was measured at four equidistant points with a ruler at
164 each flow measurement. To avoid the influence of mangrove roots on the gas fluxes, the
165 rings were placed in locations without any seedlings or aboveground mangrove roots.
166 CO_2 and CH_4 fluxes ($g\ CO_2$ or $CH_4\ m^{-2}\ d^{-1}$) were measured using the dynamic chamber
167 methodology (Norman et al., 1997; Verchot et al., 2000), sequentially connected to a
168 Los Gatos Research portable gas analyzer (Mahesh et al., 2015). The device was
169 calibrated monthly with high quality standard gas. The rings were sequentially closed
170 for three minutes with a PVC cap, which enabled the connection to the analyzer via two
171 12.0 m polyethylene hoses. The gas concentration was measured (ppm) every two
172 seconds and automatically stored by the analyzer. CO_2 and CH_4 fluxes were calculated
173 from the linear regression of increasing/decreasing CO_2 and CH_4 concentrations within
174 the chamber, usually between one and three minutes after the ring cover was placed



175 (Frankignoulle, 1988; McEwing et al., 2015). Analyzing the literature, we found that the
176 flux is considered zero when the linear regression reaches an $R^2 < 0.30$ (Sundqvist et al.,
177 2014). However, in our analyses, the vast majority of regressions reached an $R^2 > 0.70$,
178 and the regressions were weak in only 6% of the data.

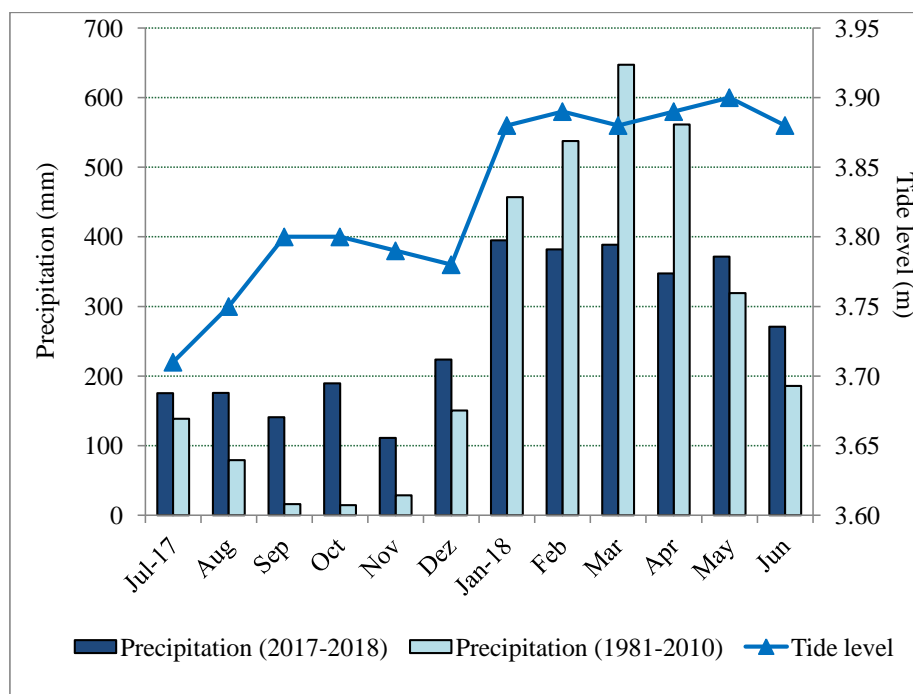
179 2.5 Statistical analyses

180 The normality of the data of FCH_4 and FCO_2 and soil physicochemical parameters was
181 determined by the Shapiro-Wilks method. The student's t-test was used to test the
182 differences ($p < 0.05$) in the emissions between the different sites and seasonal periods.
183 An ANOVA and Tukey's test ($p < 0.05$) were used when the distributions were normal.
184 For non-parametric data the Kruskal-Wallis test was used ($p < 0.05$). Pearson
185 correlation coefficients were calculated to determine the relationships between soil
186 properties and gas fluxes. Statistical analyses were performed with and free statistical
187 software Infostat 2015®.

188 3 Results

189 3.1 Precipitation

190 There was a marked seasonality during the study period (Figure 2), with 2,155.0 mm of
191 precipitation during the rainy period and 1,016.5 mm during the dry period. However,
192 the rainfall distribution was different from the climatological average (Figure 2). The
193 rainy season had 553.2 mm less precipitation, and the dry season had 589.1 mm more
194 than the climatological normal. Thus, in the period studied, the dry season was rainier,
195 and the rainy season was drier than the climatological normal.



196

197 Figure 2. Monthly climatological normal in the municipality of Soure (1981-2010, mm),
198 monthly precipitation (mm), and maximum tide height (m) for the from 2017 to 2018,
199 in the municipality of São Caetano de Odivelas (PA).

200 3.2 Carbon Dioxide and methane efflux

201 The CO₂ and CH₄ fluxes in the mangrove soil were not normally distributed, so the
202 statistical analysis was performed using a non-parametric method. CO₂ fluxes only
203 differed among topographies in January (H = 3.915; p = 0.048), July (H = 9.091; p =
204 0.003), and November (H = 11.294; p < 0.000) (Table 1), with generally higher fluxes
205 at the high topography than at the low topography. CH₄ fluxes were statistically
206 different between topographies only in November (H = 9.276; p = 0.002) and December
207 (H = 4.945; p = 0.005), with higher fluxes at the low topography (Table 1)

208 Table 1. Monthly and seasonal (dry and rainy seasons) fluxes of CO₂ and CH₄ (g CO₂ or
209 CH₄ m⁻² d⁻¹) at the high and low topographies. Numbers represent the mean (standard
210 error). Lower case letters compare topographies in the same month. Upper case letters
211 compare stations at each topography. Different boldface letters have statistically
212 significant variation (Kruskal Wallis, p < 0.05).



	CO ₂ flux (g m ⁻² d ⁻¹)		CH ₄ flux (g m ⁻² d ⁻¹)	
	High topography	Low topography	High topography	Low topography
July/2017	10.166(1.555)^a	4.036(1.027)^b	0.0724(0.0518) ^a	0.2129(0.2087) ^a
August	8.513(2.672) ^a	12.462(3.400) ^a	0.0033(0.0016) ^a	0.1270(0.1185) ^a
September	11.506(2.515) ^a	6.020(1.207) ^a	0.0014(0.0008) ^a	0.1738(0.1608) ^a
October	4.147(0.653) ^a	3.993(0.731) ^a	0.0000(0.0000) ^a	-0.0004(0.0056) ^a
November	7.648(1.064)^a	0.007(0.002)^b	-0.0004(0.0001)^b	0.1395(0.0708)^a
December	5.302(1.176) ^a	7.622(2.505) ^a	0.0009(0.0009)^b	0.1210(0.0575)^a
Dry period	7.902(0.803)^{aA}	6.202(0.895)^{bA}	0.0141(0.010)^{bB}	0.1280(0.053)^{aA}
January/2018	6.697(1.717)^a	2.995(0.493)^b	0.0007(0.0004) ^a	0.0294(0.0183) ^a
February	9.053(2.650) ^a	6.384(1.428) ^a	0.0049(0.0022) ^a	0.8743(0.7024) ^a
March	5.225(1.135) ^a	5.970(1.534) ^a	0.0077(0.0056) ^a	0.3736(0.2197) ^a
April	14.077(4.695) ^a	4.785(0.711) ^a	0.1968(0.1304) ^a	0.0372(0.2841) ^a
May	3.299(0.587) ^a	3.565(0.472) ^a	0.0014(0.0019) ^a	0.0218(0.5648) ^a
June	8.796(2.053) ^a	4.704(1.183) ^a	0.0226(0.0191) ^a	0.6739(0.6665) ^a
Rainy period	7.858(1.058) ^{aA}	4.734(0.440) ^{aA}	0.0390(0.023)^{aA}	0.3350(0.194) ^{aA}

213 At the high topography, CO₂ fluxes were significantly higher in July compared to
 214 August and December, March, October, and May, not differing from the other months
 215 of the year (H = 24.510; p = 0.011). CH₄ fluxes at the high topography were
 216 significantly (H = 40.073; p < 0.001) higher in April and July compared to the other
 217 months studied, and in November there was consumption of CH₄ from the atmosphere
 218 (Table 1). At the low topography, CO₂ fluxes were statistically (H = 19.912; p = 0.046)
 219 higher in September and February compared to January and November, not differing
 220 from the other months. CH₄ fluxes at the low topography did not show a significant
 221 variation between months (H = 10.114; p = 0.407).

222 Although seasonal CO₂ fluxes were higher at the high topography than at the low
 223 topography (Table 1), they were only statistically different in the dry season (H = 7.378;
 224 p = 0.006). In contrast, seasonal CH₄ fluxes were higher at the low topography (Table 1)
 225 but were only statistically different in the dry season (H = 8.229; p < 0.001). With this
 226 the mean annual fluxes of CO₂ and CH₄ were 6.659 ± 0.419 g CO₂ m⁻² d⁻¹ (mean ±
 227 standard error) and 0.132 ± 0.053 g CH₄ m⁻² d⁻¹, respectively.



228 3.3 Environmental characterization

229 Silt concentration was higher at the low topography (LSD: 14.763; $p=0.007$) and clay
230 concentration was higher at the high topography sites (LSD: 12.463; $p=0.005$), in both
231 stations studied (Table 2). Soil particle size analysis did not vary statistically ($p > 0.05$)
232 between the two stations (Table 2). Soil moisture did not vary significantly ($p > 0.05$)
233 between topographies at each station, or between seasonal periods at the same
234 topography (Table 2). The variable pH varied statistically only at the low topography
235 when the two stations were compared (LSD: 5.950; $p=0.006$), being more acidic in the
236 dry period (Table 2). On average pH was significantly (LSD: 0.559; $p=0.008$) higher in
237 the dry season (Table 2). No variation in Eh was identified between topographies and
238 seasons (Table 2), although it was higher in the dry season than in the rainy season.
239 However, Sal values were higher (LSD: 3.444; $p=0.010$) at the high topography than at
240 the low topography in the dry season (Table 2). In addition, Sal was significantly higher
241 in the dry season in both the high (LSD: 2.916; $p < 0.001$) and low (LSD: 3.003; $p <$
242 0.001) topographies (Table 2).



243 Table 2. Concentration analysis of Sand, Silt, Clay, Moisture, pH, Redox Potential (Eh) and salinity (Sal; ppt) in mangrove soil in the high and
 244 low topographies, and in the rainy and dry seasons, at Macaca island, São Caetano das Odivelas. Numbers represent the mean (standard error of
 245 the mean). Lower case letters compare topographies in each seasonal period, and upper-case letters compare the same topography between
 246 seasonal periods. Different letters indicate statistical variation (LSD, $p < 0.05$).

Season	Topography	Sand (%)	Silt (%)	Clay (%)	Moisture (%)	pH	Eh (mV)	Sal (ppt)
Dry	High	12.1(1.4) ^{ab}	41.8(3.3) ^{ba}	46.1(2.6) ^{ab}	73.1(6.6) ^{ab}	5.5(0.2) ^{ab}	190.25(45.53) ^{ab}	35.25(1.11) ^{ab}
	Low	9.7(2.5) ^{ab}	63.6(6.1) ^{ab}	26.6(5.2) ^{ba}	86.9(3.4) ^{ab}	5.3(0.3) ^{ab}	106.38(53.76) ^{ab}	30.13(1.16) ^{ba}
	Mean	10.9(1.4) ^A	52.7(4.4) ^A	36.4(3.8) ^A	80.0(4.0) ^A	5.4(0.2) ^A	148.31(35.71) ^A	32.69(1.02) ^A
Rainy	High	12.1(1.4) ^{ab}	41.8(3.3) ^{ba}	46.1(2.6) ^{ab}	88.9(3.5) ^{ab}	4.9(0.4) ^{ab}	92.50(56.20) ^{ab}	7.50(0.78) ^{ab}
	Low	9.7(2.5) ^{ab}	63.6(6.1) ^{ab}	26.6(5.2) ^{ba}	88.6(3.7) ^{ab}	4.4(0.1) ^{ab}	36.25(49.97) ^{ab}	8.13(0.79) ^{ab}
	Mean	10.9(1.4) ^A	52.7(4.4) ^A	36.4(3.8) ^A	88.7(2.5) ^A	4.6(0.2) ^B	64.38(37.04) ^A	7.81(0.54) ^B



248 The Cmic did not differ between topographies in the two seasons (Table 3); however
249 CT was significantly higher in the low topography in the dry season (LSD: 5.589; $p <$
250 0.000) and in the rainy season (LSD: 5.777; $p = 0.024$). In addition, Cmic was higher in
251 the dry season in both the high (LSD: 11.325; $p < 0.010$) and low (LSD: 9.345; $p <$
252 0.000) topographies (Table 3). Nmic did not vary between topographies seasonally.
253 However, Nmic in the high (LSD: 9.059; $p = 0.013$) and low topographies (LSD: 4.447;
254 $p = 0.001$) was higher during the dry season (Table 3). The C/N ratio (Table 3) was
255 higher in the low topography in both the dry (LSD: 3.142; $p < 0.000$) and rainy seasons
256 (LSD: 3.675; $p = 0.033$), when compared to the high topography. However, only in the
257 low topography was the C/N ratio higher (LSD: 1.863; $p < 0.000$) in the dry season
258 compared to the rainy season (Table 3). Soil MO was higher at the low topography in
259 the rainy (LSD: 9.950; $p = 0.024$) and in the dry seasons (LSD: 9.630; $p < 0.000$).
260 However, only in the lowland topography was the MO concentration higher in the dry
261 season than in the rainy season (Table 3).

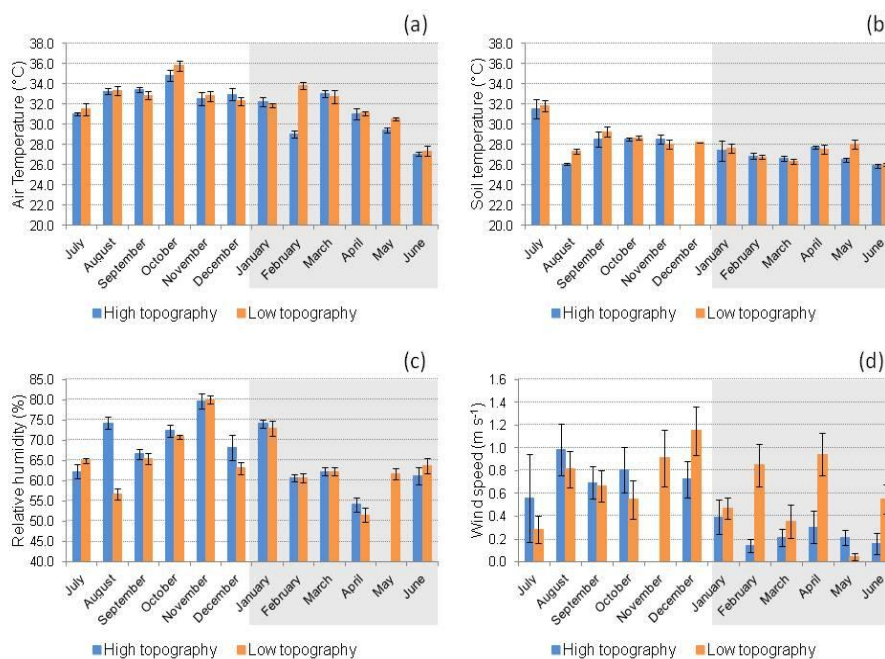


262 Table 3. Seasonal and topographic variation in microbial Carbon (C_{mic} ; $mg\ kg^{-1}$), microbial Nitrogen (N_{mic} ; $mg\ kg^{-1}$), Total Carbon (TC; $g\ kg^{-1}$)
 263 1), Total Nitrogen (NT; $g\ kg^{-1}$), Carbon/Nitrogen ratio (C/N) and Soil Organic Matter (OM; $g\ kg^{-1}$). Numbers represent the mean (standard error).
 264 Lower case letters compare topography at each station, and upper-case letters compare topography among stations.

Season	Topography	C_{mic} $mg\ kg^{-1}$	N_{mic} $mg\ kg^{-1}$	C_T $g\ kg^{-1}$	N_T $g\ kg^{-1}$	C/N	OM $g\ kg^{-1}$
Dry	High	22.12(5.22) ^{abA}	12.76(4.20) ^{abA}	14.12(2.23) ^{ba}	1.43(0.06) ^{abA}	9.60(1.20) ^{ba}	24.35(3.84) ^{ba}
	Low	26.34(4.23) ^{abA}	10.34(2.05) ^{abA}	26.44(1.35) ^{abA}	1.56(0.04) ^{abA}	16.98(0.84) ^{abA}	45.59(2.32) ^{abA}
	Mean	24.23(3.29) ^A	11.55(2.28) ^A	20.28(2.03) ^A	1.49(0.04) ^A	13.29(1.19) ^A	34.97(3.50) ^A
Rainy	High	7.40(0.79) ^{abB}	0.75(0.41) ^{abB}	11.46(2.48) ^{ba}	1.32(0.04) ^{abA}	8.42(1.70) ^{ba}	19.75(4.27) ^{ba}
	Low	5.95(1.06) ^{abB}	1.23(0.28) ^{abB}	18.27(1.06) ^{abB}	1.46(0.06) ^{abA}	12.47(0.22) ^{abB}	31.51(1.83) ^{abB}
	Mean	6.68(0.67) ^B	0.99(0.25) ^B	14.86(1.57) ^B	1.39(0.04) ^A	10.44(0.98) ^A	25.63(2.71) ^B



266 Tar was significantly higher (LSD = 0.72, $p = 0.01$) at the high topography ($31.24 \pm$
267 0.26 °C) than at the low topography (30.30 ± 0.25 °C) only in the rainy season (Figure
268 3a). No significant variation in Ts was found between the topographies in both seasons
269 (Figure 3b). The RH was significantly higher (LSD = 2.55, $p = 0.01$) at the high
270 topography ($70.54 \pm 0.97\%$) than at the low topography ($66.85 \pm 0.87\%$) only in the
271 rainy season (Figure 3c). At this same station, Vv (Figure 3d) was significantly higher
272 (LSD = 0.15, $p < 0.00$) at the low topography (0.54 ± 0.06 m s⁻¹) than at the high
273 topography (0.24 ± 0.04 m s⁻¹).



274

275 Figure 3. a) Air temperature (°C), b) soil temperature (°C), c) relative humidity (%) and
276 d) wind speed (m s⁻¹) at high and low topographies, from July 2017 to June 2018 in a
277 mangrove area in the Mojuim River estuary. Bars highlighted in grey correspond to the
278 rainy season (n = 16). The bars represent the standard error.

279 3.4 Vegetation structure and biomass

280 Only the species *R. mangle* and *A. germinans* were found in the floristic survey carried
281 out. The DBH did not vary significantly between the topographies for either species
282 (Table 4). However, *R. mangle* had a higher DBH than *A. germinaris* at both high



283 (LSD: 139.304; $p = 0.037$) and low topographies (LSD: 131.307; $p = 0.001$). The basal
284 area (BA) and AGB variables did not show significant variation (Table 4). A total
285 aboveground biomass of $322.1 \pm 49.6 \text{ Mg ha}^{-1}$ was estimated.



286 Table 4: Sum of Diameter at Breast Height (DBH), Basal Area (BA) and Above Ground Biomass (AGB) at high and low topography in the
 287 mangrove forest of the Mojuim River estuary. Numbers represent the mean (standard error of the mean). Lower case letters compare topographic
 288 height for each species, and upper-case letters compare species at each topographic height, using Tuckey's test ($p < 0.05$).

Specie	Topography	N ha ⁻¹	DBH (cm)	BA (m ² ha ⁻¹)	AGB (Mg ha ⁻¹)
<i>Rhizophora</i>	High	302.4(20.5)	238.8(24.9) ^{aA}	17.3(2.0) ^{aA}	219.3(25.7) ^{aA}
<i>mangle</i>	Low	310.4(37.6)	283.5(45.0) ^{aA}	24.2(4.3) ^{aA}	338.7(62.9) ^{aA}
<i>Avicennia</i>	High	47.7(20.5)	86.8(51.2) ^{aB}	13.8(9.2) ^{aA}	135.3(94.7) ^{aA}
<i>germinans</i>	Low	15.9(9.2)	46.1(29.3) ^{aB}	11.8(8.8) ^{aA}	136.0(108.3) ^{aA}
Total	High	350.2(18.4)	325.6(33.6) ^a	31.1(7.5) ^a	304.5(99.8) ^a
	Low	346.2(41.0)	296.0(23.7) ^a	30.0(4.1) ^a	330.8(60.4) ^a

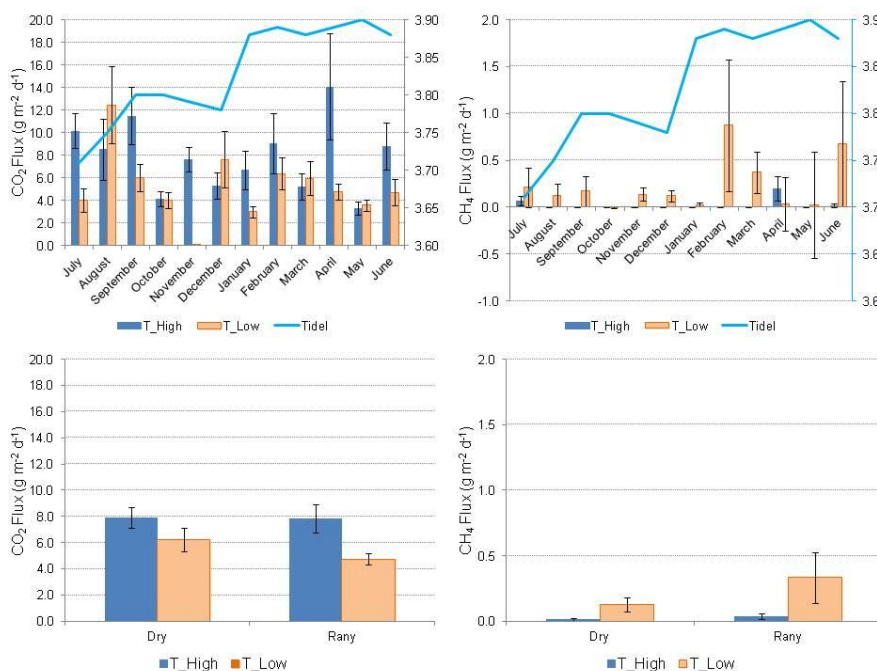
289 The equations for biomass estimates (AGB) were: $R. mangle = 0.1282 * DBH^{2.6}$, $A. germinans = 0.14 * DBH^{2.4}$, Total = $0.168 * \rho * DBH^{2.47}$, where $\rho_{R. mangle} = 0.87$; $\rho_{A. germinans} =$
 290 0.72 (Howard et al., 2014a).



291 **4 Discussion**

292 4.1 Carbon dioxide e methane flux measurements

293 It is important to consider that the year under study was rainier in the dry season and
294 less rainy in the wet season (Figure 2). Perhaps this variation is already related to the
295 effects of global climate changes. Under these conditions, the CO₂ flux from the
296 mangrove soil ranged from -5.06 to 68.96 g CO₂ m⁻² d⁻¹ (mean 6.66 g CO₂ m⁻² d⁻¹),
297 while the CH₄ flux ranged from -5.07 to 11.08 g CH₄ m⁻² d⁻¹ (mean 0.13 g CH₄ m⁻² d⁻¹),
298 resulting in a total carbon rate of 7.04 g CO₂ m⁻² d⁻¹ or 25.70 Mg CO₂ ha⁻¹ y⁻¹ (negative
299 values represent atmospheric consumption of the gas) (Figure 4). The negative CO₂ flux
300 appears to be a consequence of the increased CO₂ solubility in tidal waters, or of the
301 increased sulfate reduction (Borges et al., 2018; Chowdhury et al., 2018; Nóbrega et al.,
302 2016). The soil carbon flux in mangrove area in the Amazon region was within the
303 range of findings for other tropical mangrove areas (2.57 to 11.00 g CO₂ m⁻² d⁻¹; Shiau
304 and Chiu, 2020). However, the mean flux of 6.2 mmol CO₂ m⁻² h⁻¹ recorded in this
305 Amazonian mangrove was much higher than the mean efflux of 2.9 mmol CO₂ m⁻² h⁻¹
306 recorded in 75 mangroves during low tide periods (Alongi, 2009). We found a mean
307 monthly flux of 327.9 ± 78.0 mg CO₂ m⁻² h⁻¹ and 217.2 ± 51.0 mg CO₂ m⁻² h⁻¹, at the
308 high and low topography, respectively.



309

310 Figure 4. CO₂ and CH₄ fluxes (g CO₂ or CH₄ m⁻² d⁻¹) monthly (July 2018 to June 2019)
 311 (n = 16) and seasonally (Dry and Rany), at high (T_High) and low (T_Low)
 312 topographies (n = 96), in mangrove forest soil compared to tide level (Tidel). The bars
 313 represent the standard error of the mean.

314 An emission of 0.010 Tg CH₄ y⁻¹, 0.64 g CH₄ m⁻² d⁻¹ (Rosentreter et al., 2018b), or 26.7
 315 mg CH₄ m⁻² h⁻¹ is estimated at tropical latitudes (0 and 5°). In our study, the monthly
 316 average in CH₄ flux was higher at the low topography (7.3 ± 8.0 mg C m⁻² h⁻¹) than at
 317 the high topography (0.9 ± 0.6 mg C m⁻² h⁻¹) (Figure 4). Therefore, the CH₄-C fluxes
 318 from the mangrove soil in the Mojuim River estuary were much lower than expected.
 319 The average emission from the soil of 8.4 mmol CH₄ m⁻² d⁻¹ was well below the fluxes
 320 recorded in the Bay of Bengal, with 18.4 mmol CH₄ m⁻² d⁻¹ (Biswas et al., 2007). In the
 321 Amazonian mangrove studied the mean annual carbon equivalent efflux was 429.6 mg
 322 CO₂-eq m⁻² h⁻¹. This value is 0.00004% of the erosion losses of 103.5 Tg CO₂-eq ha⁻¹ y⁻¹
 323 projected for the next century in tropical mangrove forests (Adame et al., 2021).

324 4.2 Mangrove biomass

325 Assuming that the amount of carbon stored is 0.42 of the total biomass (Sahu and
 326 Kathiresan, 2019), the mangrove forest biomass of the Mojuim River estuary stores



327 127.9 and 138.9 Mg C ha⁻¹ at the high and low topography, respectively. This result is
328 well below the 507.8 Mg C ha⁻¹ estimated for Brazilian mangroves (Hamilton and
329 Friess, 2018), but are near the 103.7 Mg C ha⁻¹ estimated for a mangrove at Dos Guarás
330 island (Salum et al., 2020), 108.4 Mg C ha⁻¹ for the Bragantina region (Gardunho,
331 2017), and 132.3 Mg Mg C ha⁻¹ in French Guiana (Fromard et al., 1998). The estimated
332 primary production for tropical mangrove forests is 218 ± 72 Tg C y (Bouillon et al.,
333 2008). These results show that the mangroves of the Amazon estuary are more
334 productive than previously known (Bouillon et al., 2008).

335 4.3 Topography variation

336 The mangrove areas are periodically flooded, with a larger flood volume during the ebb
337 tides, especially in the rainy season. The hydrological condition of the soil is determined
338 by the microtopography and can regulate the respiration of microorganisms (aerobic or
339 anaerobic), being a decisive factor in controlling the CO₂ efflux (Dai et al., 2012;
340 Davidson et al., 2000; Ehrenfeld, 1995). In the two climatic periods of the year, the high
341 topography produced more CO₂ (7,869 ± 1,873 g CO₂ m⁻² d⁻¹) than the low topography
342 (5,212 ± 1,225 g CO₂ m⁻² d⁻¹) (Figure 4). No significant influence on CO₂ flux was
343 observed due to the low variation in high tide level throughout the year (0.19 m) (Figure
344 4), although it was numerically higher at the high topography. However, tidal height
345 and the rainy season resulted in a higher CO₂ flux (rate high/low =1.7) at the high
346 topography (7.858 ± 0.039 g CO₂ m⁻² d⁻¹) than at the low topography (4.734 ± 0.335 g
347 CO₂ m⁻² d⁻¹) (Figure 4; Table 1). This result is because the root systems of most flood-
348 tolerant plants remain active when flooded (Angelov et al., 1996). Still, the high
349 topography has longer flood-free periods, because this only happens when the tides are
350 in the form of triangle or when the rains are torrential.

351 CO₂ efflux was higher in the high topography than in the low topography, i.e., 39.8%
352 lower in the forest soil exposed to the atmosphere for less time, in the rainy season
353 (when soils are more subject to inundation). Measurements performed on 62 mangrove
354 forest soils showed an average flux of 2.87 mmol CO₂ m⁻² h⁻¹ when the soil is exposed
355 to the atmosphere, while 75 results on flooded mangrove forest soils showed an average
356 emission of 2.06 mmol CO₂ m⁻² h⁻¹ (Alongi, 2007, 2009), i.e., 28.2% less than for the
357 dry soil. Reflecting the more significant facility gases have for molecular diffusion than
358 fluids, and the increased surface area for aerobic respiration and chemical oxidation
359 during air exposure (Chen et al., 2010). Some studies attribute this variation to the



360 temperature of the soil when exposed to tropical air (Alongi, 2009), increasing the
361 export of dissolved inorganic carbon (Maher et al., 2018). However, although there was
362 no significant variation in soil temperature between topographies at each time of year
363 (Figure 3b), there was a positive correlation (Pearson = 0.15, $p = 0.05$) between CO₂
364 efflux and soil temperature at the low topography.

365 In the rainy season, CO₂ efflux was correlated with Tar (Pearson = 0.23, $p = 0.03$), RH
366 (Pearson = -0.32, $p < 0.00$) and Ts (Pearson = 0.21, $p = 0.04$) only at the low
367 topography. In the dry season CO₂ flux was correlated with Ts (Pearson = 0.39, $p <$
368 0.00) at low topography. Some studies show that CH₄ efflux is a consequence of the
369 seasonal temperature variation in mangrove forest in temperate/monsoon climate
370 (Chauhan et al., 2015; Purvaja and Ramesh, 2001; Whalen, 2005). However, in this
371 study CH₄ efflux was correlated with Ta (Pearson = -0.33, $p < 0.00$) and RH (Pearson =
372 0.28, $p = 0.01$) only in the dry season and at the low topography. These results show
373 that hardly does only one physical parameter interfere with the fluxes, and that they do
374 not interact similarly in a different topography and seasonality.

375 A compilation of several studies showed that the total CH₄ emissions from soil in
376 mangrove ecosystem range from 0 to 23.68 mg C m⁻² h⁻¹ (Shiau and Chiu, 2020), and
377 our study showed a range of -0.01 to 31.88 mg C m⁻² h⁻¹, with a mean of 4.70 ± 5.00 mg
378 C m⁻² h⁻¹. The monthly CH₄ fluxes were generally higher at the low (0.232 ± 0.256)
379 than at the high (0.026 ± 0.018) topography, especially during the high tide (Figure 4).
380 Compared to the high topography, only in the dry season was there a significantly
381 higher production at the low topography (Table 1, Figure 4). The low topography
382 produced 0.0249 g C m⁻² h⁻¹ more to the atmosphere in the rainy season than in the dry
383 season (Table 1), and the same seasonal variation was recorded in other studies
384 (Cameron et al., 2021).

385 The mangrove soil in the Mojuim River estuary is rich in silt and clay (Table 2), which
386 reduces sediment porosity and fosters the formation and retention of anoxic conditions
387 (Dutta et al., 2013). In addition, the lack of oxygen in the flooded mangrove soil
388 generates microbial processes such as denitrification, sulfate reduction, methanogenesis,
389 and redox reactions (Alongi and Christoffersen, 1992). Furthermore, plenty of the CH₄
390 produced in wetlands is dissolved in situ in the pore water caused by the high pressure,
391 which can result in supersaturation in the water, enabling CH₄ to be released from the
392 sediment to the atmosphere by diffusion and by boiling in the water (Neue et al., 1997).



393 Only the species *R. mangle* and *A. germinans* were found in the floristic survey carried
394 out, which agrees with other studies in the same region (Menezes et al., 2008). Thus, the
395 variations found in the flux between the topographies in the Mojuim River estuary are
396 not related to the mangrove forest structure because there was no significant difference
397 in the aboveground biomass. Since there was no difference in the species composition,
398 it is expected that the belowground biomass would not be different either (Table 4).

399 Soil moisture in the Mojuim River mangrove forest negatively influenced CO₂ flux in
400 both seasons (Table 5). However a correlation with the flux of CH₄ was not identified.
401 Studies show that CO₂ flux tends to be lower with high soil saturation (Chanda et al.,
402 2014; Kristensen et al., 2008). A total of 395 Mg C ha⁻¹ was found at the soil surface
403 (0.15 m) in the mangrove of the Mojuim River estuary, which was slightly higher than
404 the 340 Mg C ha⁻¹ found in mangroves in the Amazon (Kauffman et al., 2018), however
405 being significantly 1.8 times greater at the low topography (Table 3). The finer soil
406 texture at the low topography (Table 2) reduces groundwater drainage which facilitates
407 the accumulation of C in the soil (Schmidt et al., 2011).

408 4.4 Biogeochemical parameters

409 Chemical parameters of the soil were better correlated with CO₂ efflux in the dry
410 period, while the C:N ratio, OM, and Eh were correlated with CO₂ efflux in both
411 seasons (Table 5). During the seasonal and annual periods, CH₄ efflux was not
412 correlated significantly with chemical parameters (Table 5), similar to the observed in
413 another study (Chen et al., 2010). Increased soil moisture reduces gas diffusion rates,
414 which directly affects the physiological state and microbial activities, by limiting the
415 supply of the dominant electron acceptors, such as oxygen, and gases such as CH₄
416 (Blagodatsky and Smith, 2012). The importance of soil moisture was evident in the
417 richness and diversity of bacterial communities in a study comparing the different pore
418 spaces filled with water (Banerjee et al., 2016). Furthermore, sulfate reduction in
419 flooded soils (another pathway of organic matter metabolism) is dependent on the redox
420 potential of the soil. However no sulfate reduction occurs when the redox potential has
421 values above -150 mv (Connell and Patrick, 1968). In our study Eh was above 36.0 mV,
422 this indicates that sulfate reduction probably did not influence the OM metabolism.

423 On the other hand, increasing soil moisture provides the microorganisms with essential
424 substrates such as ammonium, nitrate, and soluble organic carbon, and increases gas
425 diffusion rates in the water (Blagodatsky and Smith, 2012). Biologically available



426 nitrogen often limits marine productivity (Bertics et al., 2010), and thus can affect the
427 fluxes of CO₂ to the atmosphere. A higher concentration of Cmic and Nmic in the dry
428 period (Table 3), both in the high and low topographies, indicated that microorganisms
429 are more active when the soil spends more time aerated in the dry period (Table 3), the
430 period in which the high tides produce anoxia in the mangrove soil. Additionally, the
431 C/N ratio was well below 40, indicating that soil microorganisms and roots do not
432 compete for nitrogen (Stevenson and Cole, 1999).

433 Sulfate-reducing bacteria (SO₄²⁻) are important diazotrophs in coastal ecosystems and
434 can contribute with significant nitrogen (N₂) fixation in mangrove ecosystems (Bertics
435 et al., 2010; Shiao et al., 2017; Welsh et al., 1996). The negative correlation between
436 TC, NT, C/N, and MO, along with the positive correlation of Nmic with soil CO₂ flux
437 (Table 5), in the dry period, indicates that microbial activity is a decisive factor for CO₂
438 efflux (Poungparn et al., 2009). The high MO concentration at the two topographic
439 heights (Table 3), at the two stations studied, and the respective negative correlation
440 with CO₂ flux (Table 5) confirm the importance of microbial activity in mangrove soil
441 (Gao et al., 2020). Also, CH₄ produced in flooded soils can be converted mainly to CO₂
442 by the anaerobic oxidation of CH₄ (Boetius et al., 2000; Milucka et al., 2015) which
443 may contribute to the higher CO₂ efflux in the Mojuim River estuary compared to other
444 tropical mangroves (Rosentreter et al., 2018c). The belowground C stock is considered
445 the largest C reservoir in mangrove ecosystem resulting from the low rate of OM
446 decomposition due to flooding (Marchand, 2017).



447 Table 5. Correlation coefficient (Pearson) of CO₂ and CH₄ fluxes with chemical parameters of the soil in a mangrove area in the Mojuim River
 448 estuary

Gas Flux (g m ⁻² d ⁻¹)	Season	C _T (g kg ⁻¹)	N _T (g kg ⁻¹)	C _{mic} (mg kg ⁻¹)	N _{mic} (mg kg ⁻¹)	C/N	OM (g kg ⁻¹)	Sal (ppt)	Eh (mV)	pH	Moisture (%)
CO ₂	Dry	-0.68**	-0.59*	0.18 ^{NS}	0.61**	-0.66**	-0.67**	-0.07 ^{NS}	0.51*	0.21 ^{NS}	-0.49*
	Rainy	-0.44 ^{NS}	-0.20 ^{NS}	-0.15 ^{NS}	-0.32 ^{NS}	-0.50*	-0.63**	-0.54*	0.53*	0.47 ^{NS}	-0.54*
	Annual	-0.50**	-0.35*	-0.18 ^{NS}	0.00 ^{NS}	-0.53**	-0.48**	-0.30 ^{NS}	0.39*	0.23 ^{NS}	-0.56**
CH ₄	Dry	0.30 ^{NS}	0.07 ^{NS}	-0.14 ^{NS}	-0.24 ^{NS}	0.34 ^{NS}	0.02 ^{NS}	-0.04 ^{NS}	-0.38 ^{NS}	0.26 ^{NS}	0.26 ^{NS}
	Rainy	0.05 ^{NS}	-0.09 ^{NS}	0.44 ^{NS}	-0.27 ^{NS}	0.09 ^{NS}	-0.11 ^{NS}	-0.04 ^{NS}	-0.13 ^{NS}	-0.07 ^{NS}	0.04 ^{NS}
	Annual	0.04 ^{NS}	-0.10 ^{NS}	-0.01 ^{NS}	-0.18 ^{NS}	0.08 ^{NS}	-0.01 ^{NS}	-0.17 ^{NS}	-0.21 ^{NS}	-0.08 ^{NS}	0.02 ^{NS}

449 NS= not significant; * significant effects at p ≤ 0.05; ** significant effects at p ≤ 0.01



450 The higher water salinity in the dry season (Table 2) seems to result in a lower CH₄ flux
451 at the low topography, more influenced by the tidal movement in this season (Dutta et
452 al., 2013; Lekphet et al., 2005; Shiau and Chiu, 2020). Another essential factor for the
453 reduced CH₄ emissions is when SO₄²⁻ in the brine affects the competition between SO₄²⁻
454 reduction and methanogenic fermentation, because the sulfate-reducing bacteria are
455 more efficient in hydrogen utilization than the methanotrophic bacteria (Abram and
456 Nedwell, 1978; Kristjansson et al., 1982). At high SO₄²⁻ concentrations methanotrophic
457 bacteria use CH₄ as an energy source and oxidize it to CO₂ (Coyne, 1999; Segarra et al.,
458 2015), increasing the CO₂ efflux and reducing the CH₄ efflux (Megoñigal and
459 Schlesinger, 2002; Roslev and King, 1996). This may explain the high CO₂ efflux found
460 throughout the year at the high and, especially, at the low topography (Figure 4). Only
461 in the rainy season was a significant correlation recorded between salinity and CO₂ flux.
462 Still, in all seasonal periods the correlation between salinity and CO₂ and CH₄ fluxes
463 were negative.

464 Studies in other coastal ecosystems have recorded that methanotrophic bacteria can be
465 sensitive to soil pH, and reported an optimal growth at pH ranging from 6.5 to 7.5
466 (Shiau et al., 2018). The higher soil acidity in the Mojuim River wetland (Table 2) may
467 be inhibiting the activity of methanogenic bacteria by increasing the population of
468 methanotrophic bacteria, which are efficient in consuming CH₄ (Chen et al., 2010;
469 Hegde et al., 2003; Shiau and Chiu, 2020). In addition, the pneumatophores present in
470 *R. mangle* increase soil aeration and reduce CH₄ emissions (Allen et al., 2011; He et al.,
471 2019). Spatial differences (topography) in CH₄ emissions in the soil can be attributed to
472 substrate heterogeneity, salinity, and the abundance of methanogenic and
473 methanotrophic bacteria (Gao et al., 2020). The high Eh values found in both
474 topographies, mainly in the dry period (Table 2), are unfavorable for CH₄ emission. Soil
475 Eh above -150 mV was considered limiting for CH₄ production (Yang and Chang,
476 1998). Increases in CH₄ efflux with reduced salinity were found due to intense
477 oxidation or reduced competition from the more energetically efficient SO₄²⁻ and NO₃³⁻
478 reducing bacteria than the methanogenic bacteria (Biswas et al., 2007). This fact can be
479 observed in the CH₄ efflux in the mangrove of the Mojuim River, because in the rainy
480 season (Figure 4), when there is a reduced water salinity (Table 2) due to increased
481 precipitation, there was an increased CH₄ production, especially in the low topography



482 (Figure 4). However, we did not find a correlation between CH₄ efflux and salinity, as
483 already reported (Purvaja and Ramesh, 2001)

484 No significant correlations were found between CH₄ efflux and the chemical properties
485 of the soil in the mangrove of the Mojuim River estuary (Table 5). However, with an
486 average flux of 4.70 mg C m⁻² h⁻¹ and with extreme monthly and seasonal variation,
487 more detailed studies are needed on CH₄ efflux and on the relationship with
488 methanotrophic bacteria and interactions with abiotic factors (mainly ammonia and
489 sulfate).

490 **5 Conclusions**

491 Between latitude 0° to 23.5° S the most recent estimate shows an emission of 2.3 g CO₂
492 m⁻² d⁻¹ (Rosentreter et al., 2018c). However, the efflux in the mangrove of the Mojuim
493 River estuary was 6.7 g CO₂ m⁻² d⁻¹. For the same latitudinal range, the authors
494 estimated an emission of 0.64 g CH₄ m⁻² d⁻¹, and we found an efflux of 0.13 g CH₄ m⁻²
495 d⁻¹. Seasonality was important for CH₄ efflux but did not influence CO₂ efflux. Due to
496 the rainfall variation compared to the climatology, the differences in fluxes may be an
497 effect of global climate changes on the terrestrial biogeochemistry at the plant-soil-
498 atmosphere interface, making it necessary to extend this study for more years. Using the
499 factor of 23 to convert the global warming potential of CH₄ to CO₂ (IPCC, 2001), the
500 CO₂ equivalent emission was 35.4 Mg CO_{2-eq} ha⁻¹ yr⁻¹.

501 Microtopography should be considered when determining the efflux of CO₂ and CH₄ in
502 mangrove forest in the Amazon estuary. The low topography in the mangrove forest of
503 Rio Mojuim contained a higher concentration of organic carbon in the soil. However, it
504 did not produce a higher CO₂ efflux because this was negatively influenced by soil
505 moisture, which was indifferent to CH₄ efflux. MO, C/N ratio, and Eh were critical in
506 soil microbial activity, which resulted in a variation in CO₂ flux during the year and
507 seasonal periods. In this sense, physicochemical properties of the soil are important for
508 CO₂ flux, especially in the rainy season; however, they did not influence CH₄ fluxes.

509 *Data availability:* The data used in this article belong to the doctoral thesis of Saul
510 Castellón, within the Postgraduate Program in Environmental Sciences, at the Federal
511 University of Pará. Access to the data can be requested from Dr. Castellón
512 (saularmarz22@gmail.com), which holds the set of all data used in this paper.



513 *Author contributions:* SEMC and JHC designed the study and wrote the article with the
514 help of JFB, MR, MLR, and CN. JFB assisted in the field experiment. MR provided
515 logistical support in field activities.

516 *Competing interests:* The authors declare that they have no conflict of interest

517 *Acknowledgements:* The authors are grateful to the Program of Alliances for Education
518 and Training of the Organization of the American States and to Coimbra Group of
519 Brazilian Universities, for the financial support, as well as to Paulo Sarmiento for the
520 assistance at laboratory analysis, and to Maridalva Ribeiro and Lucivaldo da Silva for
521 the fieldwork assistance. Furthermore, the authors would like to thank the Laboratory of
522 Biogeochemical Cycles (Geosciences Institute, Federal University of Pará) for the
523 equipment provided for this research.

524 **6 References**

525 Abram, J. W. and Nedwell, D. B.: Inhibition of methanogenesis by sulphate reducing
526 bacteria competing for transferred hydrogen, *Arch. Microbiol.*, 117(1), 89–92,
527 doi:10.1007/BF00689356, 1978.

528 Adame, M. F., Connolly, R. M., Turschwell, M. P., Lovelock, C. E., Fatoyinbo, T.,
529 Lagomasino, D., Goldberg, L. A., Holdorf, J., Friess, D. A., Sasmito, S. D., Sanderman,
530 J., Sievers, M., Buelow, C., Kauffman, J. B., Bryan-Brown, D. and Brown, C. J.: Future
531 carbon emissions from global mangrove forest loss, *Glob. Chang. Biol.*, 27(12), 2856–
532 2866, doi:10.1111/gcb.15571, 2021.

533 Allen, D., Dalal, R. C., Rennenberg, H. and Schmidt, S.: Seasonal variation in nitrous
534 oxide and methane emissions from subtropical estuary and coastal mangrove sediments,
535 Australia, *Plant Biol.*, 13(1), 126–133, doi:10.1111/j.1438-8677.2010.00331.x, 2011.

536 Almeida, R. F. de, Mikhael, J. E. R., Franco, F. O., Santana, L. M. F. and Wendling, B.:
537 Measuring the labile and recalcitrant pools of carbon and nitrogen in forested and
538 agricultural soils: A study under tropical conditions, *Forests*, 10(7), 544,
539 doi:10.3390/f10070544, 2019.

540 Alongi, D. M.: The contribution of mangrove ecosystems to global carbon cycling and
541 greenhouse gas emissions, in *Greenhouse gas and carbon balances in mangrove coastal
542 ecosystems*, edited by Y. Tateda, R. Upstill-Goddard, T. Goreau, D. M. Alongi, A.
543 Nose, E. Kristensen, and G. Wattayakorn, pp. 1–10, Gendai Tosho, Kanagawa, Japan.,



- 544 2007.
- 545 Alongi, D. M.: The energetics of mangrove forests, Springer., 2009.
- 546 Alongi, D. M. and Christoffersen, P.: Benthic infauna and organism-sediment relations
547 in a shallow, tropical coastal area: influence of outwelled mangrove detritus and
548 physical disturbance, *Mar. Ecol. Prog. Ser.*, 81(3), 229–245, doi:10.3354/meps081229,
549 1992.
- 550 Alongi, D. M. and Mukhopadhyay, S. K.: Contribution of mangroves to coastal carbon
551 cycling in low latitude seas, *Agric. For. Meteorol.*, 213, 266–272,
552 doi:10.1016/j.agrformet.2014.10.005, 2015.
- 553 Angelov, M. N., Sung, S. J. S., Doong, R. Lou, Harms, W. R., Kormanik, P. P. and
554 Black, C. C.: Long-and short-term flooding effects on survival and sink-source
555 relationships of swamp-adapted tree species, *Tree Physiol.*, 16(4), 477–484,
556 doi:10.1093/treephys/16.5.477, 1996.
- 557 Araujo, A. S. F. de: Is the microwave irradiation a suitable method for measuring soil
558 microbial biomass?, *Rev. Environ. Sci. Biotechnol.*, 9(4), 317–321,
559 doi:10.1007/s11157-010-9210-y, 2010.
- 560 Banerjee, S., Helgason, B., Wang, L., Winsley, T., Ferrari, B. C. and Siciliano, S. D.:
561 Legacy effects of soil moisture on microbial community structure and N₂O emissions,
562 *Soil Biol. Biochem.*, 95, 40–50, doi:10.1016/j.soilbio.2015.12.004, 2016.
- 563 Bastviken, D., Tranvik, L. J., Downing, J. A., Crill, P. M. and Enrich-Prast, A.:
564 Freshwater Methane Emissions Offset the Continental Carbon Sink, *Science* (80-.),
565 331(6013), 50–50, doi:10.1126/science.1196808, 2011.
- 566 Bauza, J. F., Morell, J. M. and Corredor, J. E.: Biogeochemistry of Nitrous Oxide
567 Production in the Red Mangrove (*Rhizophora mangle*) Forest Sediments, *Estuar. Coast.
568 Shelf Sci.*, 55(5), 697–704, doi:10.1006/ECSS.2001.0913, 2002.
- 569 Bertics, V. J., Sohm, J. A., Treude, T., Chow, C. E. T., Capone, D. G., Fuhrman, J. A.
570 and Ziebis, W.: Burrowing deeper into benthic nitrogen cycling: The impact of
571 Bioturbation on nitrogen fixation coupled to sulfate reduction, *Mar. Ecol. Prog. Ser.*,
572 409, 1–15, doi:10.3354/meps08639, 2010.
- 573 Biswas, H., Mukhopadhyay, S. K., Sen, S. and Jana, T. K.: Spatial and temporal
574 patterns of methane dynamics in the tropical mangrove dominated estuary, NE coast of



- 575 Bay of Bengal, India, *J. Mar. Syst.*, 68(1–2), 55–64, 2007.
- 576 Blagodatsky, S. and Smith, P.: Soil physics meets soil biology: Towards better
577 mechanistic prediction of greenhouse gas emissions from soil, *Soil Biol. Biochem.*, 47,
578 78–92, doi:10.1016/J.SOILBIO.2011.12.015, 2012.
- 579 Boetius, A., Ravensschlag, K., Schubert, C. J., Rickert, D., Widdel, F., Gleseke, A.,
580 Amann, R., Jørgensen, B. B., Witte, U. and Pfannkuche, O.: A marine microbial
581 consortium apparently mediating anaerobic oxidation methane, *Nature*, 407(6804), 623–
582 626, doi:10.1038/35036572, 2000.
- 583 Borges, A. V., Abril, G., Darchambeau, F., Teodoru, C. R., Deborde, J., Vidal, L. O.,
584 Lambert, T. and Bouillon, S.: Divergent biophysical controls of aquatic CO₂ and CH₄
585 in the World’s two largest rivers, *Sci. Rep.*, 5, doi:10.1038/srep15614, 2015.
- 586 Borges, A. V., Abril, G. and Bouillon, S.: Carbon dynamics and CO₂ and CH₄
587 outgassing in the Mekong delta, *Biogeosciences*, 15(4), doi:10.5194/bg-15-1093-2018,
588 2018.
- 589 Bouillon, S., Borges, A. V., Castañeda-Moya, E., Diele, K., Dittmar, T., Duke, N. C.,
590 Kristensen, E., Lee, S. Y., Marchand, C., Middelburg, J. J., Rivera-Monroy, V. H.,
591 Smith, T. J. and Twilley, R. R.: Mangrove production and carbon sinks: A revision of
592 global budget estimates, *Global Biogeochem. Cycles*, 22(2),
593 doi:10.1029/2007GB003052, 2008.
- 594 Brookes, P. C., Landman, A., Pruden, G. and Jenkinson, D. S.: Chloroform fumigation
595 and the release of soil nitrogen: A rapid direct extraction method to measure microbial
596 biomass nitrogen in soil, *Soil Biol. Biochem.*, 17(6), 837–842, doi:10.1016/0038-
597 0717(85)90144-0, 1985.
- 598 Cameron, C., Hutley, L. B., Munksgaard, N. C., Phan, S., Aung, T., Thinn, T., Aye, W.
599 M. and Lovelock, C. E.: Impact of an extreme monsoon on CO₂ and CH₄ fluxes from
600 mangrove soils of the Ayeyarwady Delta, Myanmar, *Sci. Total Environ.*, 760, 143422,
601 doi:10.1016/J.SCITOTENV.2020.143422, 2021.
- 602 Chanda, A., Akhand, A., Manna, S., Dutta, S., Das, I., Hazra, S., Rao, K. H. and
603 Dadhwal, V. K.: Measuring daytime CO₂ fluxes from the inter-tidal mangrove soils of
604 Indian Sundarbans, *Environ. Earth Sci.*, 72(2), 417–427, doi:10.1007/s12665-013-2962-
605 2, 2014.



- 606 Chauhan, R., Datta, A., Ramanathan, A. and Adhya, T. K.: Factors influencing spatio-
607 temporal variation of methane and nitrous oxide emission from a tropical mangrove of
608 eastern coast of India, *Atmos. Environ.*, 107, 95–106,
609 doi:10.1016/j.atmosenv.2015.02.006, 2015.
- 610 Chen, G. C., Tam, N. F. Y. and Ye, Y.: Spatial and seasonal variations of atmospheric
611 N₂O and CO₂ fluxes from a subtropical mangrove swamp and their relationships with
612 soil characteristics, *Soil Biol. Biochem.*, 48, 175–181,
613 doi:10.1016/j.soilbio.2012.01.029, 2012.
- 614 Chen, G. C. C., Tam, N. F. Y. F. Y. and Ye, Y.: Summer fluxes of atmospheric
615 greenhouse gases N₂O, CH₄ and CO₂ from mangrove soil in South China, *Sci. Total*
616 *Environ.*, 408(13), 2761–2767, doi:10.1016/j.scitotenv.2010.03.007, 2010.
- 617 Chowdhury, T. R., Bramer, L., Hoyt, D. W., Kim, Y. M., Metz, T. O., McCue, L. A.,
618 Diefenderfer, H. L., Jansson, J. K. and Bailey, V.: Temporal dynamics of CO₂ and CH₄
619 loss potentials in response to rapid hydrological shifts in tidal freshwater wetland soils,
620 *Ecol. Eng.*, 114, 104–114, doi:10.1016/j.ecoleng.2017.06.041, 2018.
- 621 Connell, W. E. and Patrick, W. H.: Sulfate reduction in soil: Effects of redox potential
622 and pH, *Science (80-.)*, 159(3810), 86–87, doi:10.1126/science.159.3810.86, 1968.
- 623 Coyne, M.: *Soil Microbiology: An Exploratory Approach*, Delmar Publishers, New
624 York, NY, USA., 1999.
- 625 Dai, Z., Trettin, C. C., Li, C., Li, H., Sun, G. and Amatya, D. M.: Effect of Assessment
626 Scale on Spatial and Temporal Variations in CH₄, CO₂, and N₂O Fluxes in a Forested
627 Wetland, *Water, Air, Soil Pollut.*, 223(1), 253–265, doi:10.1007/s11270-011-0855-0,
628 2012.
- 629 Davidson, E. A., Verchot, L. V., Cattanio, J. H., Ackerman, I. L. and Carvalho, J. E. M.:
630 Effects of soil water content on soil respiration in forests and cattle pastures of eastern
631 Amazonia, *Biogeochemistry*, 48(1), 53–69, doi:10.1023/a:1006204113917, 2000.
- 632 Donato, D. C., Kauffman, J. B., Murdiyarso, D., Kurnianto, S., Stidham, M. and
633 Kanninen, M.: Mangroves among the most carbon-rich forests in the tropics, *Nat.*
634 *Geosci.*, 4(5), 293–297, doi:10.1038/ngeo1123, 2011.
- 635 Dutta, M. K., Chowdhury, C., Jana, T. K. and Mukhopadhyay, S. K.: Dynamics and
636 exchange fluxes of methane in the estuarine mangrove environment of the Sundarbans,



- 637 NE coast of India, *Atmos. Environ.*, 77, 631–639, doi:10.1016/j.atmosenv.2013.05.050,
638 2013.
- 639 Ehrenfeld, J. G.: Microsite differences in surface substrate characteristics in
640 *Chamaecyparis* swamps of the New Jersey Pinelands, *Wetlands*, 15(2), 183–189,
641 doi:10.1007/BF03160672, 1995.
- 642 El-Robrini, M., Alves, M. A. M. S., Souza Filho, P. W. M., El-Robrini M. H. S., Silva
643 Júnior, O. G. and França, C. F.: Atlas de Erosão e Progradação da zona costeira do
644 Estado do Pará – Região Amazônica: Áreas oceânica e estuarina, in Atlas de Erosão e
645 Progradação da Zona Costeira Brasileira, edited by D. Muehe, pp. 1–34, São Paulo.,
646 2006.
- 647 EPA, E. P. A.: Inventory of U.S. Greenhouse Gas Emissions and Sinks: 1990–2015.,
648 2017.
- 649 Fernandes, W. A. A. and Pimentel, M. A. da S.: Dinâmica da paisagem no entorno da
650 RESEX marinha de São João da Ponta/PA: utilização de métricas e geoprocessamento,
651 *Caminhos Geogr.*, 20(72), 326–344, doi:10.14393/RCG207247140, 2019.
- 652 Ferreira, A. S., Camargo, F. A. O. and Vidor, C.: Utilização de microondas na avaliação
653 da biomassa microbiana do solo, *Rev. Bras. Ciência do Solo*, 23(4), 991–996,
654 doi:10.1590/S0100-06831999000400026, 1999.
- 655 Ferreira, S. da S.: Entre marés e mangues: paisagens territorializadas por pescadores da
656 resex marinha de São João da Ponta/PA /, Universidade Federal do Pará., 2017.
- 657 França, C. F. de, Pimentel, M. A. D. S. and Neves, S. C. R.: Estrutura Paisagística De
658 São João Da Ponta, Nordeste Do Pará, *Geogr. Ensino Pesqui.*, 20(1), 130,
659 doi:10.5902/2236499418331, 2016.
- 660 Frankignoulle, M.: Field measurements of air-sea CO₂ exchange', *Limnol. Oceanogr.*,
661 33(3), 313–322, 1988.
- 662 Friesen, S. D., Dunn, C. and Freeman, C.: Decomposition as a regulator of carbon
663 accretion in mangroves: a review, *Ecol. Eng.*, 114, 173–178,
664 doi:10.1016/j.ecoleng.2017.06.069, 2018.
- 665 Fromard, F., Puig, H., Cadamuro, L., Marty, G., Betoulle, J. L. and Mougin, E.:
666 Structure, above-ground biomass and dynamics of mangrove ecosystems: new data
667 from French Guiana, *Oecologia*, 115(1), 39–53, doi:10.1007/s004420050489, 1998.



- 668 Gao, G. F., Zhang, X. M., Li, P. F., Simon, M., Shen, Z. J., Chen, J., Gao, C. H. and
669 Zheng, H. L.: Examining Soil Carbon Gas (CO₂, CH₄) Emissions and the Effect on
670 Functional Microbial Abundances in the Zhangjiang Estuary Mangrove Reserve, J.
671 Coast. Res., 36(1), 54–62, doi:10.2112/JCOASTRES-D-18-00107.1, 2020.
- 672 Gardunho, D. C. .: Estimativas de biomassa acima do solo da floresta de mangue na
673 península de Ajuruteua, Bragança – PA, Unversidade Federal do Pará., 2017.
- 674 Hamilton, S. E. and Friess, D. A.: Global carbon stocks and potential emissions due to
675 mangrove deforestation from 2000 to 2012, Nat. Clim. Chang., 8(3),
676 doi:10.1038/s41558-018-0090-4, 2018.
- 677 He, Y., Guan, W., Xue, D., Liu, L., Peng, C., Liao, B., Hu, J., Zhu, Q., Yang, Y., Wang,
678 X., Zhou, G., Wu, Z. and Chen, H.: Comparison of methane emissions among invasive
679 and native mangrove species in Dongzhaigang, Hainan Island, Sci. Total Environ., 697,
680 133945, doi:10.1016/j.scitotenv.2019.133945, 2019.
- 681 Hegde, U., Chang, T.-C. and Yang, S.-S.: Methane and carbon dioxide emissions from
682 Shan-Chu-Ku landfill site in northern Taiwan., Chemosphere, 52(8), 1275–1285,
683 doi:10.1016/S0045-6535(03)00352-7, 2003.
- 684 Herz, R.: Manguezais do Brasil, Instituto Oceanografico da Usp/Cirm, São Paulo,
685 Brazil., 1991.
- 686 Howard, J., Hoyt, S., Isensee, K., Telszewski, M. and Pidgeon, E., Eds.: Coastal blue
687 Carbon: Methods for assessing carbon stocks and emissions factors in mangroves, tidal
688 salt marshes, and seagrasses, International Union for Conservation of Nature, Arlington,
689 Virginia, USA. [online] Available from: www.ioc.unesco.org (Accessed 11 September
690 2019a), 2014.
- 691 Howard, J., Hoyt, S., Isensee, K., Telszewski, M. and Pidgeon, E.: Coastal Blue
692 Carbon: Methods for Assessing Carbon Stocks and Emissions Factors in Mangroves,
693 Tidal Salt Marshes, and Seagrasses, Arlington, Virginia, USA. [online] Available from:
694 [http://www.unesco.org/new/en/natural-sciences/ioc-oceans/sections-and-](http://www.unesco.org/new/en/natural-sciences/ioc-oceans/sections-and-programmes/ocean-sciences/ocean-carbon/coastal-blue-carbon/)
695 [programmes/ocean-sciences/ocean-carbon/coastal-blue-carbon/](http://www.unesco.org/new/en/natural-sciences/ioc-oceans/sections-and-programmes/ocean-sciences/ocean-carbon/coastal-blue-carbon/), 2014b.
- 696 IPCC: Climate Change 2001: Third Assessment Report of the IPCC, Cambridge., 2001.
- 697 Islam, K. R. and Weil, R. R.: Microwave irradiation of soil for routine measurement of
698 microbial biomass carbon, Biol. Fertil. Soils, 27(4), 408–416,



- 699 doi:10.1007/s003740050451, 1998.
- 700 Kalembasa, S. J. and Jenkinson, D. S.: A comparative study of titrimetric and
701 gvimetric methods for determination of organic carbon in soil, *J. Sci. Food Agric.*, 24,
702 1085–1090, 1973.
- 703 Kauffman, B. J., Donato, D. and Adame, M. F.: Protocolo para la medición, monitoreo
704 y reporte de la estructura, biomasa y reservas de carbono de los manglares, Bogor,
705 Indonesia., 2013.
- 706 Kauffman, J. B., Bernardino, A. F., Ferreira, T. O., Giovannoni, L. R., De Gomes, L. E.
707 O., Romero, D. J., Jimenez, L. C. Z. and Ruiz, F.: Carbon stocks of mangroves and salt
708 marshes of the Amazon region, Brazil, *Biol. Lett.*, 14(9), doi:10.1098/rsbl.2018.0208,
709 2018.
- 710 Kristensen, E., Bouillon, S., Dittmar, T. and Marchand, C.: Organic carbon dynamics in
711 mangrove ecosystems: A review, *Aquat. Bot.*, 89(2), 201–219,
712 doi:10.1016/J.AQUABOT.2007.12.005, 2008.
- 713 Kristjansson, J. K., Schönheit, P. and Thauer, R. K.: Different K_s values for hydrogen
714 of methanogenic bacteria and sulfate reducing bacteria: An explanation for the apparent
715 inhibition of methanogenesis by sulfate, *Arch. Microbiol.*, 131(3), 278–282,
716 doi:10.1007/BF00405893, 1982.
- 717 Lekphet, S., Nitorisavut, S. and Adsavakulchai, S.: Estimating methane emissions from
718 mangrove area in Ranong Province, Thailand, *Songklanakarin J. Sci. Technol.*, 27(1),
719 153–163 [online] Available from: <https://www.researchgate.net/publication/26473398>
720 (Accessed 29 January 2019), 2005.
- 721 Maher, D. T., Call, M., Santos, I. R. and Sanders, C. J.: Beyond burial: Lateral
722 exchange is a significant atmospheric carbon sink in mangrove forests, *Biol. Lett.*,
723 14(7), 1–4, doi:10.1098/rsbl.2018.0200, 2018.
- 724 Mahesh, P., Sreenivas, G., Rao, P. V. N., Dadhwal, V. K., Sai Krishna, S. V. S. and
725 Mallikarjun, K.: High-precision surface-level CO₂ and CH₄ using off-axis integrated
726 cavity output spectroscopy (OA-ICOS) over Shadnagar, India, *Int. J. Remote Sens.*,
727 36(22), 5754–5765, doi:10.1080/01431161.2015.1104744, 2015.
- 728 Marchand, C.: Soil carbon stocks and burial rates along a mangrove forest
729 chronosequence (French Guiana), *For. Ecol. Manage.*, 384, 92–99,



- 730 doi:10.1016/j.foreco.2016.10.030, 2017.
- 731 McEwing, K. R., Fisher, J. P. and Zona, D.: Environmental and vegetation controls on
732 the spatial variability of CH₄ emission from wet-sedge and tussock tundra ecosystems
733 in the Arctic, *Plant Soil*, 388(1–2), 37–52, doi:10.1007/s11104-014-2377-1, 2015.
- 734 Megonigal, J. P. and Schlesinger, W. H.: Methane-limited methanotrophy in tidal
735 freshwater swamps, *Global Biogeochem. Cycles*, 16(4), 35-1-35–10,
736 doi:10.1029/2001GB001594, 2002.
- 737 Menezes, M. P. M. de, Berger, U. and Mehlig, U.: Mangrove vegetation in Amazonia :
738 a review of studies from the coast of Pará and Maranhão States , north Brazil, *Acta*
739 *Amaz.*, 38(3), 403–420, doi:10.1590/S0044-59672008000300004, 2008.
- 740 Milucka, J., Kirf, M., Lu, L., Krupke, A., Lam, P., Littmann, S., Kuypers, M. M. M. and
741 Schubert, C. J.: Methane oxidation coupled to oxygenic photosynthesis in anoxic
742 waters, *ISME J.*, 9(9), 1991–2002, doi:10.1038/ismej.2015.12, 2015.
- 743 Monz, C. A., Reuss, D. E. and Elliott, E. T.: Soil microbial biomass carbon and nitrogen
744 estimates using 2450 MHz microwave irradiation or chloroform fumigation followed by
745 direct extraction, *Agric. Ecosyst. Environ.*, 34(1–4), 55–63, doi:10.1016/0167-
746 8809(91)90093-D, 1991.
- 747 Neue, H. U., Gaunt, J. L., Wang, Z. P., Becker-Heidmann, P. and Quijano, C.: Carbon
748 in tropical wetlands, in *Geoderma*, vol. 79, pp. 163–185, Elsevier., 1997.
- 749 Nóbrega, G. N., Ferreira, T. O., Siqueira Neto, M., Queiroz, H. M., Artur, A. G.,
750 Mendonça, E. D. S., Silva, E. D. O. and Otero, X. L.: Edaphic factors controlling
751 summer (rainy season) greenhouse gas emissions (CO₂ and CH₄) from semiarid
752 mangrove soils (NE-Brazil), *Sci. Total Environ.*, 542, 685–693,
753 doi:10.1016/j.scitotenv.2015.10.108, 2016.
- 754 Norman, J. M., Kucharik, C. J., Gower, S. T., Baldocchi, D. D., Crill, P. M., Rayment,
755 M., Savage, K. and Striegl, R. G.: A comparison of six methods for measuring
756 soil-surface carbon dioxide fluxes, *J. Geophys. Res. Atmos.*, 102(D24), 28771–28777,
757 doi:10.1029/97JD01440@10.1002/(ISSN)2169-8996.BOREAS2, 1997.
- 758 Peel, M. C., Finlayson, B. L. and McMahon, T. A.: Updated world map of the Köppen-
759 Geiger climate classification, *Hydrol. Earth Syst. Sci.*, 11(5), 1633–1644,
760 doi:10.1002/ppp.421, 2007.



- 761 Poffenbarger, H. J., Needelman, B. A. and Megonigal, J. P.: Salinity Influence on
762 Methane Emissions from Tidal Marshes, Wetlands, 31(5), 831–842,
763 doi:10.1007/s13157-011-0197-0, 2011.
- 764 Pongparn, S., Komiyama, A., Tanaka, A., Sangtiewan, T., Maknual, C., Kato, S.,
765 Tanapermpool, P. and Patanaponpaiboon, P.: Carbon Dioxide Emission through Soil
766 Respiration in a Secondary Mangrove Forest of Eastern Thailand, Source J. Trop. Ecol.,
767 25(4), 393–400, doi:10.1017/S0266467409006154, 2009.
- 768 Prost, M. T., Mendes, A. C., Faure, J. F., Berredo, J. F., Sales, M. E. ., Furtado, L. G.,
769 Santana, M. G., Silva, C. A., Nascimento, I. ., Gorayeb, I., Secco, M. F. and Luz, L.:
770 Manguezais e estuários da costa paraense: exemplo de estudo multidisciplinar integrado
771 (Marapanim e São Caetano de Odivelas), in Ecossistemas costeiros: impactos e gestão
772 ambiental, edited by M. T. Prost and A. Mendes, pp. 25–52, FUNTEC and Museu
773 Paraense Emílio Goeldi, Belém, Brazil., 2001.
- 774 Purvaja, R. and Ramesh, R.: Natural and Anthropogenic Methane Emission from
775 Coastal Wetlands of South India, Environ. Manage., 27(4), 547–557,
776 doi:10.1007/s002670010169, 2001.
- 777 Purvaja, R., Ramesh, R. and Frenzel, P.: Plant-mediated methane emission from an
778 Indian mangrove, Glob. Chang. Biol., 10(11), 1825–1834, doi:10.1111/j.1365-
779 2486.2004.00834.x, 2004.
- 780 Reeburgh, W. S.: Oceanic Methane Biogeochemistry, Chem. Rev., 2, 486–513,
781 doi:10.1021/cr050362v, 2007.
- 782 Robertson, A. I., Alongi, D. M. and Boto, K. G.: Food chains and carbon fluxes, in
783 Coastal and Estuarine Studies, edited by A. I. Robertson and D. M. Alongi, pp. 293–
784 326, American Geophysical Union. [online] Available from:
785 [https://books.google.com.br/books?hl=pt-BR&lr=&id=-
786 uGA_Kpcr04C&oi=fnd&pg=PP7&dq=Tropical+Mangrove+Ecosystems&ots=bi4Rqwc
787 Rhv&sig=KiIbq_4NOBONARwOfblqo8YVSdI&redir_esc=y#v=onepage&q=Tropical
788 Mangrove Ecosystems&f=false](https://books.google.com.br/books?hl=pt-BR&lr=&id=-uGA_Kpcr04C&oi=fnd&pg=PP7&dq=Tropical+Mangrove+Ecosystems&ots=bi4RqwcRhv&sig=KiIbq_4NOBONARwOfblqo8YVSdI&redir_esc=y#v=onepage&q=Tropical) (Accessed 22 July 2020), 1992.
- 789 Rocha, A. S.: Caracterização física do estuário do rio Mojuim em São Caetano de
790 Odivelas - Pa, Universidade Federal do Pará., 2015.
- 791 Rollnic, M., Costa, M. S., Medeiros, P. R. L. and Monteiro, S. M.: Tide Influence on



- 792 Suspended Matter Transport in an Amazonian Estuary, *J. Coast. Res.*, 85(85 (10085)),
793 121–125, doi:10.2112/SI85-025.1, 2018.
- 794 Rosentreter, J. A., Maher, D. T. T., Erler, D. V. V., Murray, R. and Eyre, B. D. D.:
795 Factors controlling seasonal CO₂ and CH₄ emissions in three tropical mangrove-
796 dominated estuaries in Australia, *Estuar. Coast. Shelf Sci.*, 215(October), 69–82,
797 doi:10.1016/j.ecss.2018.10.003, 2018a.
- 798 Rosentreter, J. A., Maher, D. T., Erler, D. V., Murray, R. H. and Eyre, B. D.: Methane
799 emissions partially offset “blue carbon” burial in mangroves, *Sci. Adv.*, 4(6), eaao4985,
800 doi:10.1126/sciadv.aao4985, 2018b.
- 801 Rosentreter, J. A., Maher, D. . T., Erler, D. V. V., Murray, R. and Eyre, B. D. D.:
802 Seasonal and temporal CO₂ dynamics in three tropical mangrove creeks – A revision of
803 global mangrove CO₂ emissions, *Geochim. Cosmochim. Acta*, 222, 729–745,
804 doi:10.1016/j.gca.2017.11.026, 2018c.
- 805 Roslev, P. and King, G. M.: Regulation of methane oxidation in a freshwater wetland by
806 water table changes and anoxia, *FEMS Microbiol. Ecol.*, 19(2), 105–115,
807 doi:10.1111/j.1574-6941.1996.tb00203.x, 1996.
- 808 Sahu, S. K. and Kathiresan, K.: The age and species composition of mangrove forest
809 directly influence the net primary productivity and carbon sequestration potential,
810 *Biocatal. Agric. Biotechnol.*, 20, 101235, doi:10.1016/j.bcab.2019.101235, 2019.
- 811 Salum, R. B., Souza-Filho, P. W. M., Simard, M., Silva, C. A., Fernandes, M. E. B.,
812 Cougo, M. F., do Nascimento, W. and Rogers, K.: Improving mangrove above-ground
813 biomass estimates using LiDAR, *Estuar. Coast. Shelf Sci.*, 236(June 2019), 106585,
814 doi:10.1016/j.ecss.2020.106585, 2020.
- 815 Schmidt, M. W. I., Torn, M. S., Abiven, S., Dittmar, T., Guggenberger, G., Janssens, I.
816 A., Kleber, M., Kögel-Knabner, I., Lehmann, J., Manning, D. A. C., Nannipieri, P.,
817 Rasse, D. P., Weiner, S. and Trumbore, S. E.: Persistence of soil organic matter as an
818 ecosystem property, *Nature*, 478(7367), 49–56, doi:10.1038/nature10386, 2011.
- 819 Segarra, K. E. A., Schubotz, F., Samarkin, V., Yoshinaga, M. Y., Hinrichs, K. U. and
820 Joye, S. B.: High rates of anaerobic methane oxidation in freshwater wetlands reduce
821 potential atmospheric methane emissions, *Nat. Commun.*, 6(1), 1–8,
822 doi:10.1038/ncomms8477, 2015.



- 823 Shiau, Y. J. and Chiu, C. Y.: Biogeochemical processes of C and N in the soil of
824 mangrove forest ecosystems, *Forests*, 11(5), 1–15, doi:10.3390/F11050492, 2020.
- 825 Shiau, Y. J., Lin, M. F., Tan, C. C., Tian, G. and Chiu, C. Y.: Assessing N₂ fixation in
826 estuarine mangrove soils, *Estuar. Coast. Shelf Sci.*, 189, 84–89,
827 doi:10.1016/j.ecss.2017.03.005, 2017.
- 828 Shiau, Y. J., Cai, Y., Lin, Y. Te, Jia, Z. and Chiu, C. Y.: Community Structure of Active
829 Aerobic Methanotrophs in Red Mangrove (*Kandelia obovata*) Soils Under Different
830 Frequency of Tides, *Microb. Ecol.*, 75(3), 761–770, doi:10.1007/s00248-017-1080-1,
831 2018.
- 832 Souza Filho, P. W. M.: Costa de manguezais de macromaré da Amazônia: cenários
833 morfológicos, mapeamento e quantificação de áreas usando dados de sensores remotos,
834 *Rev. Bras. Geofísica*, 23(4), 427–435, doi:10.1590/S0102-261X2005000400006, 2005.
- 835 Sparling, G. P. and West, A. W.: A direct extraction method to estimate soil microbial
836 C: calibration in situ using microbial respiration and ¹⁴C labelled cells, *Soil Biol.*
837 *Biochem.*, 20(3), 337–343, doi:10.1016/0038-0717(88)90014-4, 1988.
- 838 Stevenson, F. J. and Cole, M. A.: *Cycles of Soils: Carbon, Nitrogen, Phosphorus,*
839 *Sulfur, Micronutrients*, 2nd Editio., Wiley, New York, NY, USA. [online] Available
840 from: [https://www.wiley.com/en-](https://www.wiley.com/en-us/Cycles+of+Soils%3A+Carbon%2C+Nitrogen%2C+Phosphorus%2C+Sulfur%2C+Micronutrients%2C+2nd+Edition-p-9780471320715)
841 [us/Cycles+of+Soils%3A+Carbon%2C+Nitrogen%2C+Phosphorus%2C+Sulfur%2C+M](https://www.wiley.com/en-us/Cycles+of+Soils%3A+Carbon%2C+Nitrogen%2C+Phosphorus%2C+Sulfur%2C+Micronutrients%2C+2nd+Edition-p-9780471320715)
842 [icronutrients%2C+2nd+Edition-p-9780471320715](https://www.wiley.com/en-us/Cycles+of+Soils%3A+Carbon%2C+Nitrogen%2C+Phosphorus%2C+Sulfur%2C+Micronutrients%2C+2nd+Edition-p-9780471320715) (Accessed 27 May 2021), 1999.
- 843 Sundqvist, E., Vestin, P., Crill, P., Persson, T. and Lindroth, A.: Short-term effects of
844 thinning, clear-cutting and stump harvesting on methane exchange in a boreal forest,
845 *Biogeosciences*, 11(21), 6095–6105, doi:10.5194/bg-11-6095-2014, 2014.
- 846 Valentim, M., Monteiro, S. and Rollnic, M.: The Influence of Seasonality on Haline
847 Zones in An Amazonian Estuary, *J. Coast. Res.*, 85, 76–80, doi:10.2112/SI85-016.1,
848 2018.
- 849 Valentine, D. L.: Emerging Topics in Marine Methane Biogeochemistry, *Ann. Rev.*
850 *Mar. Sci.*, 3(1), 147–171, doi:10.1146/annurev-marine-120709-142734, 2011.
- 851 Vance, E. D., Brookes, P. C. and Jenkinson, D. S.: An extraction method for measuring
852 soil microbial biomass C, *Soil Biol. Biochem.*, 19(6), 703–707, doi:10.1016/0038-
853 0717(87)90052-6, 1987.



854 Verchot, L. V., Davidson, E. A., Cattânio, J. H. and Ackerman, I. L.: Land-use change
855 and biogeochemical controls of methane fluxes in soils of eastern Amazonia,
856 *Ecosystems*, 3(1), 41–56, doi:10.1007/s100210000009, 2000.

857 Welsh, D. T., Bourgués, S., De Wit, R. and Herbert, R. A.: Seasonal variations in
858 nitrogen-fixation (acetylene reduction) and sulphate-reduction rates in the rhizosphere
859 of *Zostera noltii*: Nitrogen fixation by sulphate-reducing bacteria, *Mar. Biol.*, 125(4),
860 619–628, doi:10.1007/BF00349243, 1996.

861 Whalen, S. C.: Biogeochemistry of Methane Exchange between Natural Wetlands and
862 the Atmosphere, *Environ. Eng. Sci.*, 22(1), 73–94, doi:10.1089/ees.2005.22.73, 2005.

863 Yang, S. S. and Chang, H. L.: Effect of environmental conditions on methane
864 production and emission from paddy soil, *Agric. Ecosyst. Environ.*, 69(1), 69–80,
865 doi:10.1016/S0167-8809(98)00098-X, 1998.

866